$E = 7$ meV; has a spatial wavelength of $\sim 4.2 \pm 0.4a_0$; and is between 10 and 100 times as intense as the modulations near $E = 7$ meV (with a different wavevector) discussed in this study. There is a possibility that the field-induced "checkerboard" could be produced by quasiparticle scattering off the vortex core, or it could be an indirect signature of a second-order parameter stabilized near the core, or it could even be some combination of the two. New experiments will be required to distinguish between these cases.

A third issue is the range of coherent quasiparticle interference patterns and the imprecise location of their scattering centers. The smallest $\vec{q}$-space extent of an FT(E,$\vec{q}$) peak in Fig. 3 is $\Delta q \sim 0.1\pi/a_0$. This indicates that the longest coherence length for any modulation is $\ell \sim 80$ Å. Several phenomena such as gap disorder [with patch size ~30 Å (*23–26*)], impurity resonances (with spacing of ~100 Å visible in Fig. 2B), or oxygen atoms (with spacing of ~13 Å at this nominal doping) may influence this coherence length. We cannot at present identify which factors are key.

The fourth, and possibly most important, point is that quasiparticle scattering between high joint-DOS regions of $\vec{k}$-space has now received direct experimental support as a mechanism for incommensurate, dispersive, spatial modulations of the superconducting electronic structure. A related process, in which a quasiparticle is scattered across the Fermi energy into a quasi-hole and vice versa, has been theoretically discussed as a potential explanation (*11–14*) for the incommensurate, dispersive, magnetic phenomena detected by neutron scattering in the cuprates (*30*). Renewed exploration of such a scattering-related explanation for these phenomena may therefore be appropriate.

References and Notes

1. M. F. Crommie, C. P. Lutz, D. M. Eigler, *Nature* **363**, 524 (1993).
2. Y. Hasegawa, P. Avouris, *Phys. Rev. Lett.* **71**, 1071 (1993).
3. L. Bürgi, H. Brune, O. Jeandupeux, K. Kern, *J. Electron Spectrosc. Relat. Phenom.* **109**, 33 (2000).
4. Chr. Wittneven, R. Dombrowski, M. Morgenstern, R. Wiesendanger, *Phys. Rev. Lett.* **81**, 5616 (1998).
5. K. Kanisawa, M. J. Butcher, H. Yamaguchi, Y. Hirayama, *Phys. Rev. Lett.* **86**, 3384 (2001).
6. A. Yazdani, B. A. Jones, C.P. Lutz, M. F. Crommie, D. M. Eigler, *Science* **275**, 1767 (1997).
7. D. J. Derro *et al.*, *Phys. Rev. Lett.* **88**, 97002 (2002).
8. J. M. Byers, M. E. Flatté, D. J. Scalapino, *Phys. Rev. Lett.* **71**, 3363 (1993).
9. L. Petersen, Ph. Hofmann, E. W. Plummer, F. Besenbacher, *J. Electron Spectrosc. Relat. Phenom.* **109**, 97 (2000).
10. D. Fujita *et al.*, *Surf. Sci.* **423**, 160 (1999).
11. Q. Si, Y. Zha, J. P. Liu, *Phys. Rev. B* **47**, 9055 (1993).
12. P. B. Littlewood, J. Zaanen, G. Aeppli, H. Monien, *Phys. Rev. B* **48**, 487 (1993).
13. J. Brinckman, P. A. Lee, *Phys. Rev. Lett.* **82**, 2915 (1999).
14. M. R. Norman, *Phys. Rev. B* **61**, 14751 (2000).
15. D. S. Dessau *et al.*, *Phys. Rev. Lett.* **71**, 2781 (1993).
16. Z. X. Shen *et al.*, *Science* **267**, 5196 (1995).
17. H. Ding *et al.*, *Phys. Rev. B* **54**, R9678 (1996).
18. M. R. Norman *et al.*, *Nature* **392**, 157 (1998)
19. T. Valla *et al.*, *Science* **285**, 2110 (1999).
20. D. L. Feng *et al.*, *Science* **289**, 277 (2000).
21. J. Mesot *et al.*, *Phys. Rev. Lett.* **83**, 840 (1999).
22. J. Corson *et al.*, *Phys. Rev. Lett.* **85**, 2569 (2000).
23. T. Cren, D. Roditchev, W. Sacks, J. Klein, *Europhys. Lett.* **54**, 84 (2001).
24. S. H. Pan *et al.*, *Nature* **413**, 282 (2001).
25. C. Howald, P. Fournier, A. Kapitulnik, *Phys. Rev. B* **64**, 100504 (2001).
26. K. M. Lang *et al.*, *Nature* **415**, 412 (2002).
27. Q.-H. Wang, D.-H. Lee, *Condens. Matter.*, in press (preprint available at xxx.lanl.gov/abs/cond-mat/0205118).
28. C. Howald, H. Eisaki, N. Kaneko, A. Kapitulnik, *Condens. Matter.*, in press (preprint available at xxx.lanl.gov/abs/cond-mat/0201546).
29. J. E. Hoffman *et al.*, *Science* **295**, 466 (2002).
30. H. A. Mook, P. Dai, F. Doğan, *Phys. Rev. Lett.* **88**, 97004 (2002).
31. We especially thank K. Selby for proposing the analysis scheme, E. Hudson for the software upon which its implementation is based, R. Simmonds for help with the analysis, and J. Orenstein for advice and encouragement. We acknowledge and thank J. C. Campuzano, P. Johnson, S. Kivelson, A. Lanzara, R. B. Laughlin, C. Lupien, M. Norman, S. Sachdev, and Z.-X. Shen for helpful conversations and communications. This project was supported by the National Science Foundation, the Office of Naval Research, the LDRD Program of Lawrence Berkeley National Laboratory, NEDO, and by Grant-in-Aids and a COE Grant from the Ministry of Education (Japan). J.E.H. acknowledges support by a Hertz Fellowship and K.M.L. acknowledges support by an IBM Fellowship.

8 April 2002; accepted 13 June 2002

Direct Evidence for a Marine Source of C_1 and C_2 Alkyl Nitrates

Adele L. Chuck,* Suzanne M. Turner, Peter S. Liss

Alkyl nitrates are a significant component of the "odd nitrogen" reservoir and play an important role in regulating tropospheric ozone levels in remote marine regions. Measurements of methyl and ethyl nitrate in seawater and air samples along two Atlantic Ocean transects provide the first direct evidence for an oceanic source of these compounds. Equatorial surface waters were highly supersaturated (up to 800%) in both species, with the waters in the temperate regions generally being closer to equilibrium. A simple box model calculation suggests that the equatorial source could be a major component of the local atmospheric alkyl nitrate budget.

The oxidizing capacity of the troposphere reflects the ability of the atmosphere to cleanse itself of anthropogenic and natural compounds. It is primarily determined by the concentration of hydroxyl radicals (OH), which are formed mainly from the photodissociation of ozone by ultraviolet radiation. Photolysis of oxidized nitrogen species ($NO_x = NO_2 + NO$) is the only known way of producing ozone in the troposphere (*1*); therefore, the photochemical processes occurring in the lower atmosphere are critically dependent on the level of NO_x. NO_x is short-lived and is converted into a range of organic and inorganic species, such as peroxyacetyl nitrate (PAN, $CH_3C(O)OONO_2$), peroxynitric acid ($HOONO_2$), dinitrogen pentoxide (N_2O_5), alkyl nitrate ($RONO_2$), chlorine nitrate ($ClONO_2$), nitric acid (HNO_3), nitrous acid (HNO_2), and aerosol nitrate (NO_3^-). The collective name for these compounds is "odd nitrogen" (NO_y). The alkyl nitrates ($RONO_2$) are a significant component of the odd nitrogen reservoir (NO_y) (*2–5*) and, along with the other chemically labile components of NO_y, play an important role in regulating the levels of tropospheric ozone in remote marine regions, where the typically low levels of NO_x lead to a close balance between the formation and destruction of tropospheric ozone.

After the discovery of the light alkyl nitrates in the atmosphere (*6*), the source of these compounds was assumed to be exclusively anthropogenic, via primary emissions from combustion and chemical processes and secondary formation from atmospheric photooxidation of organic compounds in the presence of NO_x (*7*). In the remote atmosphere, the concentration of methyl nitrate ($MeONO_2$) is expected to be low because of low concentrations of NO_x and a branching ratio of less than 1% for the formation of $MeONO_2$ from the reaction of alkylperoxy radicals with NO (*8*). However, unexpectedly high levels of $RONO_2$ in marine air and observations of a strong positive correlation between ethyl and propyl nitrate and the marine biogenically produced halocarbon, bromoform, in the marine boundary layer over the equatorial Pacific Ocean led Atlas *et al.* to propose an oceanic source for alkyl nitrates in the atmosphere (*9*). Subsequent atmospheric sampling campaigns, mostly conducted over the remote Pacific Ocean, have provided yet more evi-

---

School of Environmental Sciences, University of East Anglia, Norwich, Norfolk, NR4 7TJ, UK.

*To whom correspondence should be addressed. E-mail: a.chuck@uea.ac.uk

dence to support the hypothesis of an oceanic source (*2*, *10*), with the contribution of alkyl nitrates to the NO_y sum reaching 80% in equatorial and high-latitude regions over the South Pacific (*10*). Although there have been no published measurements confirming the oceanic emission of these species, other studies have also invoked a seawater source for methyl, ethyl, and propyl nitrates (*11*, *12*).

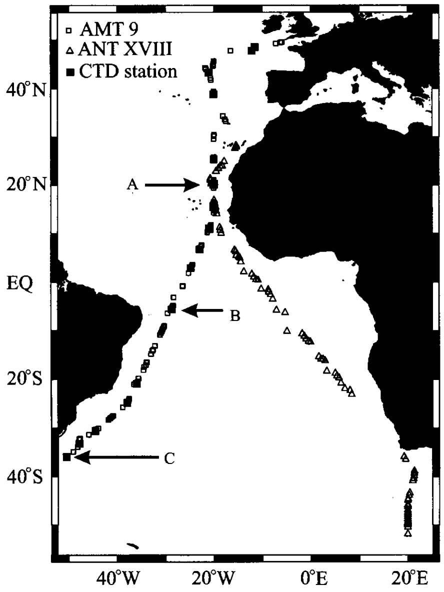

Fig. 1. Cruise tracks of the RRS *James Clark Ross* (AMT 9) and RV *Polarstern* (ANT XVIII/1). Open symbols show the positions of surface water samples; solid symbols show the positions of the CTD stations during AMT 9. A, B, and C are the positions of the depth profiles discussed in the text.

In order to investigate the hypothesis that the ocean is a source of the light alkyl nitrates, we made measurements of $MeONO_2$ and ethyl nitrate ($EtONO_2$) in seawater and air samples along two north-south transects in the Atlantic Ocean. The first was part of the 9th Atlantic Meridional Transect (AMT) cruise aboard the Royal Research Ship (RRS) *James Clark Ross* (15 September to 13 October 1999; from Grimsby, UK, to Montevideo, Uruguay), and the second was aboard the Research Vessel (RV) *Polarstern* (ANT XVIII/1, 29 September to 23 October 2000; from Bremerhaven, Germany, to Cape Town, South Africa). Figure 1 shows the surface water sampling positions during both cruises and the positions of the depth profiles taken during AMT 9 (*13*). Water and air samples were analyzed on board with a purge-and-trap gas chromatographic system with electron capture detection (GC-ECD) (*14*). Quantification of the compounds was carried out after the cruises with the use of liquid standards prepared in our laboratory. During the cruises, a stored secondary standard was analyzed twice daily to account for any changes in the detector sensitivity.

Surface seawater concentrations of $MeONO_2$ ranged from 0.15 to 2.59 ng liter^{-1} (mean, 0.49 ng liter^{-1}; median, 0.33 ng liter^{-1}) during AMT 9 (Fig. 2A), and 0.01 to 17.49 ng liter^{-1} (mean, 3.66 ng liter^{-1}; median, 1.78 ng liter^{-1}) during ANT XVIII/1 (Fig. 2B). The two cruise tracks diverged south of 10°N, and the mean concentration of $MeONO_2$ was significantly higher on the eastern side of the Atlantic. Because the time of year of sampling was similar for both cruises, it is likely that this difference was due to the closer proximity to the African coast during the ANT XVIII/1 cruise and the possible influence of coastal upwelling (*15*) on the alkyl nitrate concentrations. A notable feature seen during both cruises was the elevated concentrations of $MeONO_2$ measured close to the equator. Concentrations of $EtONO_2$ were lower than those of $MeONO_2$, ranging from 0.07 to 1.93 ng liter^{-1} (mean, 0.33 ng liter^{-1}; median, 0.35 ng liter^{-1}) during AMT 9 (Fig. 2D), and 0.12 to 3.05 ng liter^{-1} (mean, 0.83 ng liter^{-1}; median, 0.48 ng liter^{-1}) during ANT XVIII/1 (Fig. 2E). Concentrations of $EtONO_2$ were higher in the eastern Atlantic, as was also found for $MeONO_2$. The surface distribution of $EtONO_2$ mirrored that of $MeONO_2$ during both cruises, and statistical analysis of the entire surface water data set (Spearman's rank correlation) resulted in a positive correlation (the relative abundance of $MeONO_2$ to $EtONO_2$ is approximately 4:1) with an R^2 of 0.78 (n = 170 surface water samples), possibly suggesting similar mechanisms of production for both compounds. The surface water distributions shown in Fig. 2, A and D, appear to exhibit a U-shaped trend for both $MeONO_2$ and $EtONO_2$, with higher concentrations being found in the higher latitudes, possibly indicative of a relationship between alkyl nitrate production and sea surface temperature.

The atmospheric mole fraction of $MeONO_2$ ranged from 1.2 to 43 pptv (parts per trillion by volume = 10^{-12}) (Fig. 2, A and B) and 0.8 to 10 pptv for $EtONO_2$ (Fig. 2, D and E). These values lie within the range of concentrations reported in the literature for $MeONO_2$ (0.2 to 50

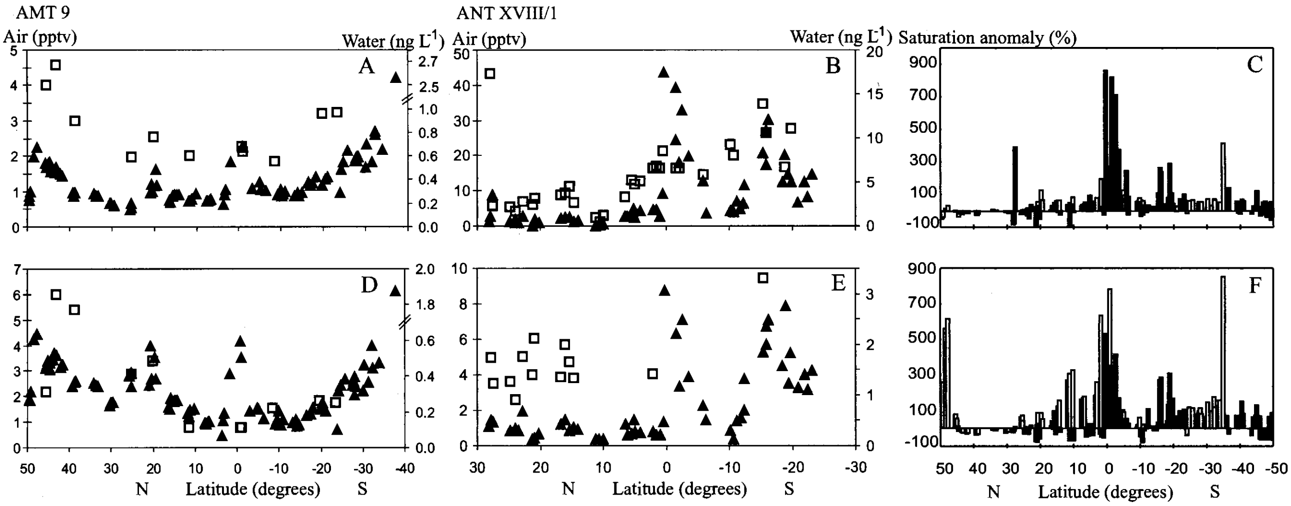

Fig. 2. Surface water concentrations, air concentrations, and saturation anomalies for $MeONO_2$ and $EtONO_2$ in the Atlantic Ocean. Surface seawater (▲) and air (□) concentrations of $MeONO_2$ (**A** and **B**) and $EtONO_2$ (**D** and **E**) during AMT 9 and ANT XVIII/1 are shown. Data are plotted against latitude, where positive values are degrees north and negative values are degrees south. During AMT 9, the final sampling point of the transect resulted in the highest surface water concentrations for both compounds, and although this sample was not from continental shelf waters, chlorophyll a concentrations were elevated and it is likely that the waters were influenced by runoff from the Rio Plata. A scale break on the water concentration axis has been used for clarity. Saturation anomalies for $MeONO_2$ (**C**) and $EtONO_2$ (**F**), calculated from the measured surface seawater and air concentrations during AMT 9 (open bars) and ANT XVIII/1 (solid bars) are shown. Positive saturation anomalies represent a net efflux from the ocean, and vice versa.

pptv) and $EtONO_2$ (0.3 to 12.2 pptv) in the remote marine troposphere (*2*, *8*, *9*). For each surface water sample, the degree of saturation of each compound was calculated by means of the measured air concentration (*16*) and the temperature-dependent Henry's law constant (H_c) (*17*). The supersaturation of surface waters over large areas of the Atlantic provides the first direct evidence for an oceanic source of $MeONO_2$ and $EtONO_2$ (Fig. 2, C and F). The equatorial region, in particular, appears to be a strong source region, with saturation anomalies (*18*) reaching 800% for both compounds. In the more temperate oceanic regions, particularly in the Northern Hemisphere, concentrations in the surface ocean appear to be near equilibrium with the overlying atmosphere, suggesting that some areas of the ocean may constitute a sink for the alkyl nitrates.

The net sea-to-air flux of the alkyl nitrates has been calculated with the use of the measured saturation anomaly, the transfer velocity parameterization of Nightingale *et al.* (*19*), and 10-min averages of wind speed, recorded at the time of sample collection. To highlight the large spatial variability of the alkyl nitrate fluxes, the mean flux per 20° of latitude between 60°N and 60°S has been calculated (Table 1). It can be seen from the table that the dominant source region is found between the equator and 40°S. For the first approximation of the potential total oceanic flux of the alkyl nitrates, we have assumed that the predominant source region is found within the latitudinal range spanning the equator and 40°S. The average flux of $MeONO_2$ for this area, based on the two data sets, is ~119 nmol m^{-2} day^{-1}. The area of ocean within these boundaries is ~2.67×10^{13} m^2. Therefore, the annual flux would be approximately 9×10^{10} g $year^{-1}$. If the equatorial Pacific Ocean is also assumed to be a source region, as could be inferred from the atmospheric measurements of methyl nitrate collected by Blake *et al.* (*10*), the annual flux is increased to 23×10^{10} g $year^{-1}$. For $EtONO_2$, the equivalent fluxes are 2.6×10^{10} g $year^{-1}$ and 6.8×10^{10} g $year^{-1}$ for the equatorial Atlantic and Pacific, respectively (*20*). These calculations have a large degree of uncertainty associated with them because of the limited data. Although it is not possible to provide a precise estimate of the uncertainty, an indication of the range of fluxes, calculated using different parameterizations of gas transfer, is given in (*20*).

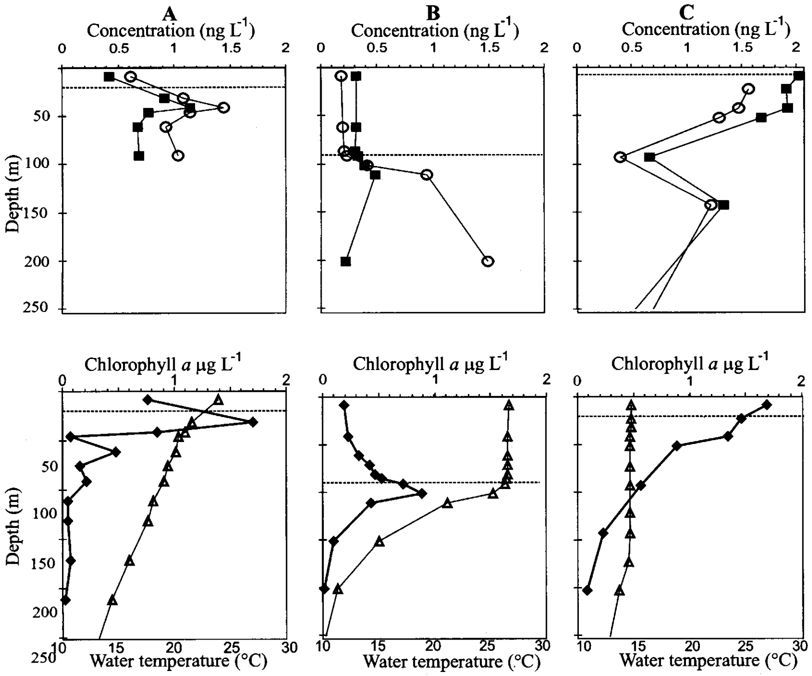

Fig. 3. Depth profiles of $MeONO_2$ (■) and $EtONO_2$ (○) (top) and chlorophyll a (◆) and water temperature (△) (bottom) at three stations along the AMT 9 cruise. Station A (20.119°N, 20.0041°W), station B (5.6532°S, 28.3414°W), and station C (36.0015°S, 50.5049°W) are shown. The dotted line indicates the mixed layer depth, which was determined by visual inspection of the temperature profiles collected during the CTD casts. The mixed layer was deep in the subtropical gyre and shallow at station C, which was influenced by runoff from the Rio Plata.

Table 1. Mean fluxes in nmol m^{-2} day^{-1} for $MeONO_2$ and $EtONO_2$ calculated for each 20° of latitude along both Atlantic Ocean transects. Negative values represent a mean flux into the ocean; positive values represent a mean efflux from the ocean. A dash indicates that there were no measurements for the alkyl nitrates in a particular latitudinal band.

Latitude (°)	AMT (nmol m^{-2} day^{-1})		ANT XVII/1I (nmol m^{-2} day^{-1})	
	$MeONO_2$	$EtONO_2$	$MeONO_2$	$EtONO_2$
60°–40°N	−22	13	–	–
40°–20°N	0	1	−58	−12
20°–0°N	7	7	29	−1
0°–20°S	13	5	231	50
20°–40°S	20	15	142	35
40°–60°S	–	–	83	−1

The demonstration of an oceanic source for $MeONO_2$ and $EtONO_2$ raises some important issues that will need to be addressed, not least their mode of formation in seawater. No mechanisms for the production of alkyl nitrates in aquatic systems or, indeed, in any biological system are known. However, depth profiles measured during the AMT 9 cruise (Fig. 3) provide some clues to possible production mechanisms. Although the strong correlation between surface water concentrations suggests a common origin, from the depth profiles it appears that distinct mechanisms may be responsible for the production of methyl and ethyl nitrate, with different water types supporting different mechanisms. The AMT cruise track crosses a range of ecosystems, including temperate waters, upwelling regions, the tropics, and subtropical gyres. The AMT program is such that there exists for this transect an extensive characterization, both spatially and temporally, of the physical and biological features found along it (*21*). At station A (Fig. 3A), sampled in the Canary Current Upwelling region (CCUp), maximum concentrations of $MeONO_2$ and $EtONO_2$ coincided with the chlorophyll maximum, indicating a biological source. In a profile from the South Atlantic subtropical gyre (Fig. 3B), high concentrations of $EtONO_2$ deep in the water column (below 100 m) suggest that production was likely to be due to bacterial and/or algal processes. Similarities in the depth profiles of $EtONO_2$ and the dissolved nutrient NO_3^- were seen in the majority of depth profiles, which may indicate a role for NO_3^- ions in the formation of this particular compound. Methyl nitrate generally showed profiles more typically associated with algal production, with decreasing concentrations below the chlorophyll maximum. In contrast, in waters more strongly affected by continental influences, such as increased loading of dissolved organic matter, the alkyl nitrates showed maximum concentrations in surface waters, which may suggest that photochemical production is important in shelf and coastal regions (Fig. 3C).

To try to highlight the importance of oceanic fluxes of alkyl nitrates to the atmosphere, we have calculated the atmospheric residence time of $MeONO_2$ and $EtONO_2$. Use of the mean sea-to-air fluxes for 0° to 40°S (Table 1) and measured atmospheric concentrations results in a lifetime of between 4.5 and 25 days for $MeONO_2$ and between 5 and 10 days for $EtONO_2$ (*22*). Literature estimates of the atmospheric lifetime of $MeONO_2$, based on known atmospheric destruction processes, are poorly constrained, ranging from 6 to 29 days (*23*, *24*). For $EtONO_2$, the atmospheric lifetime with respect to photodissociation at the equator and at 40°S has been estimated to be 7 and 12 days, respectively, for October (*25*). The reasonable agreement between the two methods implies that, for this region at least, the oceanic flux of these light alkyl nitrates is a significant source component of the light alkyl nitrate budget, thereby satisfying the requirements of the reported atmospheric measurements for a marine source.

References and Notes

1. R. P. Wayne, *Chemistry of Atmospheres* (Clarendon, Oxford, 1991).
2. R. W. Talbot, *et al.*, *J. Geophys. Res.* **105**, 6681 (2000).
3. M. Schneider, K. Ballschmiter, *Chemosphere* **38**, 233 (1999).
4. A. E. Jones *et al.*, *J. Geophys. Res.* **104**, 21355 (1999).
5. D. A. Day, P. J. Wooldridge, M. B. Dillon, J. A. Thornton, R. C. Cohen, *J. Geophys. Res.* **107** (2002).
6. E. Atlas, *Nature* **331**, 426 (1988).
7. J. M. Roberts, *Atmos. Environ.* **24A**, 243 (1990).
8. R. Atkinson, S. M. Aschmann, A. M. Winer, *J. Atmos. Chem.* **5**, 91 (1987).
9. E. Atlas, W. Pollock, J. Greenberg, L. Heidt, *J. Geophys. Res.* **98**, 16933 (1993).
10. N. J. Blake *et al.*, *J. Geophys. Res.* **104**, 21803 (1999).
11. H. Singh *et al.*, *Nature* **410**, 1078 (2001).
12. H. P. McIntyre, thesis, University of East Anglia, Norwich, UK (2001).
13. Surface water samples, taken from the ship's pumped nontoxic supplies, were collected at 2- to 4-hour intervals in 100-ml gas-tight glass syringes. Seawater was pumped from a depth of ~7 m during AMT 9 and ~11 m during ANT XVIII/1. During AMT 9, daily depth profiles were also carried out, in which seawater samples were collected from Niskin bottles mounted on a Seabird conductivity temperature depth (CTD) rosette. Air samples, collected in conjunction with surface water samples, were pumped into 3-liter electropolished stainless steel cylinders from the bow of the ship (~15 m above sea level) when the wind direction was within ± 90° of the bow, in order to avoid contamination from the ship's stack.
14. Water samples (40 ml) were typically analyzed within 4 hours of collection. During depth profiling, samples were unavoidably stored for up to 10 hours and were kept in the dark under running seawater. Air samples (600 ml) were analyzed within 2 hours of collection. Both sample types were injected into the same volatile extraction and preconcentration system. The volatile compounds were concentrated on an empty stainless steel sampling loop (30 cm length, 0.03" internal diameter) positioned above the temperature-controlled headspace of a liquid nitrogen–filled dewar. The analytes were injected onto the GC column (DB 624, 60 m length, 0.53 mm outer diameter, and 3 μm phase thickness) by heating the trap to ~100°C using boiling water. The column was temperature-programmed from 35° to 150°C. Tests for purging and trap efficiency, detector linearity, and storage artefacts were performed on board. Peak precision for $MeONO_2$ and $EtONO_2$ was better than 11%, based on the analysis of triplicate seawater samples.
15. J. R. E. Lutjeharms, P. L. Stockton, *S. Afr. J. Mar. Sci.* **5**, 35 (1987).
16. Air sampling was carried out less frequently than seawater sampling. A linear interpolation procedure was used to estimate atmospheric concentrations when no paired air and water concentrations were available. Chromatographic problems during ANT XVIII/1 resulted in very few measurements of $EtONO_2$, particularly in the Southern Hemisphere.
17. Temperature-dependent H_c's for the alkyl nitrates in seawater were determined experimentally in our laboratory using the McAuliffe technique (*26*). The temperature-dependent equations obtained were $\ln H_c = -4427/T + 11.48$ for $MeONO_2$ and $\ln H_c = -4137/T + 10.78$ for $EtONO_2$, where T is temperature.
18. The saturation anomaly (in percent) is defined as the departure of the observed dissolved amount from equilibrium saturation anomaly (%) =
$$100\left(\frac{[\text{water}]-[\text{air}]/H_c}{[\text{air}]/H_c}\right)$$
19. P. D. Nightingale *et al.*, *Global Biogeochem. Cycles* **14**, 373 (2000).
20. These estimates are sensitive to the value of the transfer velocity (k). The relationship of Nightingale *et al.* (*16*) was used in this work, because it was considered to be the most up-to-date parameterization. The fluxes would be lowered by approximately 30% had the relationship of Liss and Merlivat (1986) (*27*) been used in the calculations and increased by 15% had the parameterization of Wannikhof (1992) (*28*) been used. In a similar calculation, but using the temperature-dependent H_c's of Kames and Schurath (1992) (*29*) instead of our values, we find the mean flux calculated for the ocean area between the equator and 40°S to be 56 nmol m^{-2} day^{-1}; that is, approximately half of the ~119 nmol m^{-2} day^{-1} reported above. This highlights the importance of obtaining accurate data for the H_c's of these compounds in seawater over a range of water temperatures.
21. J. Aiken *et al.*, *Progr. Oceanogr.* **45**, 257 (2000).
22. A simple box model was used to calculate the residence time of $RONO_2$. The box represents a 1-m^2 area of the tropical ocean, overlain by the marine boundary layer, which was taken to be 1 km thick.
23. M. P. Turberg *et al.*, *J. Photochem. Photobiol. A Chem.* **51**, 281 (1990).
24. J. Williams, thesis, University of East Anglia, Norwich, UK (1994).
25. K. C. Clemitshaw *et al.*, *J. Photochem. Photobiol. A Chem.* **102**, 117 (1997).
26. C. McAuliffe, *Chem. Tec.* **1**, 46 (1971).
27. P. S. Liss, L. Merlivat, in *The Role of Sea-Air Exchange in Geochemical Cycling*, P. Buat-Menard, Ed. (Reidel, Dordrecht, Netherlands, 1986), pp. 113–127).
28. R. Wanninkof, *J. Geophys. Res.* **97**, 7373 (1992).
29. J. Kames, U. Schurath, *J. Atmos. Chem.* **15**, 79 (1992).
30. A.L.C. was funded by a Natural Environmental Research Council Studentship (GT04/98/75/MS). We thank K. Clemitshaw for donating pure solutions of methyl nitrate and ethyl nitrate, H. Wilson for collecting and analyzing the chlorophyll a data during AMT 9, and the officers and crews of the RRS *James Clark Ross* and RV *Polarstern*. We also thank two anonymous reviewers for their helpful comments.

13 May 2002; accepted 9 July 2002

Subduction and Recycling of Nitrogen Along the Central American Margin

Tobias P. Fischer,[1]* David R. Hilton,[2] Mindy M. Zimmer,[1] Alison M. Shaw,[2] Zachary D. Sharp,[1] James A. Walker[3]

We report N and He isotopic and relative abundance characteristics of volatiles emitted from two segments of the Central American volcanic arc. In Guatemala, $\delta^{15}N$ values are positive (i.e., greater than air) and N_2/He ratios are high (up to 25,000). In contrast, Costa Rican N_2/He ratios are low (maximum 1483) and $\delta^{15}N$ values are negative (minimum –3.0 per mil). The results identify shallow hemipelagic sediments, subducted into the Guatemalan mantle, as the transport medium for the heavy N. Mass balance arguments indicate that the subducted N is efficiently cycled to the atmosphere by arc volcanism. Therefore, the subduction zone acts as a "barrier" to input of sedimentary N to the deeper mantle.

The present-day isotopic composition of N (*1*) is different in the various terrestrial reservoirs. For example, the mantle supplying mid-ocean ridge basalts (MORB) is depleted [$\delta^{15}N \sim -5$ per mil (‰)] compared with Earth's atmosphere (*2–7*). The isotopic difference between mantle and atmospheric N was probably established early in Earth's history, reflecting the integrated effects of partial outgassing of primordial N, possible late addition of asteroidal and/or cometary N, and/or hydrodynamic escape of a primary atmosphere (*8–11*). Subsequent modifications to the N isotope balance between the mantle and atmosphere may have occurred through subduction of biogenic and terrigenous sediments into the mantle (*12*). Sedimentary material also has a N isotopic composition ($\delta^{15}N \sim +6$ to $+7$‰) distinct from the atmosphere and upper mantle (*13*, *14*) resulting from a kinetic isotope effect that has enriched (residual) nitrate in ^{15}N (*15–17*). This large isotopic contrast between mantle and crustal/atmospheric reservoirs gives N potential as a tracer of volatile recycling between the surface and Earth's interior. Here we focus on volatile exchange associated with the sub-

---

[1] Department of Earth and Planetary Sciences, University of New Mexico, Albuquerque, NM 87131, USA. [2] Fluids and Volatiles Laboratory, Geosciences Research Division, Scripps Institution of Oceanography, La Jolla, CA 92093, USA. [3] Department of Geology and Environmental Sciences, Northern Illinois University, DeKalb, IL 60115, USA.

*To whom correspondence should be addressed. E-mail: fischer@unm.edu